

Supplementary Information

Precisely Engineered Conjugated Polyimide Cathode with Dense Redox-Active Carbonyl Sites for Superior Lithium-Ion Battery Performance

*Mohamed A. Elnaggar, Nanxi Dong, Yongjun Kang, Bingxue Liu, Daolei Lin, Guofeng Tian, Shengli Qi, * Dezhen Wu*

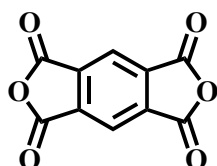
Calculation of the theoretical capacity

Theoretical specific capacity (mA h g^{-1}) of any redox material was obtained through the following equation:¹

$$C_{\text{spec}} = \frac{n \times F}{3.6 \times M_w} \quad (\text{S1})$$

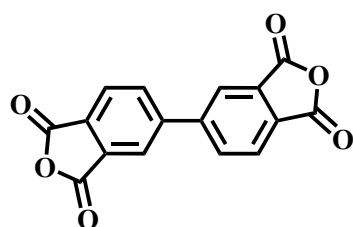
Where n refers to the number of transferred electrons in each repeating unit, F is the Faraday constant (96485 C mol^{-1}), and M_w stands for the molecular weight of a structural repeating unit of redox-active material. Consequently, the theoretical capacities of our materials are as follows:

(1) The theoretical capacity of PMDA is 245 m Ah g^{-1} , where its chemical structure is as follows:



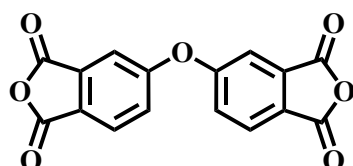
Molecular Weight = $218.12 \text{ g mol}^{-1}$

(2) The theoretical capacity of BPDA is 182 m Ah g^{-1} , where its chemical structure is as follows:



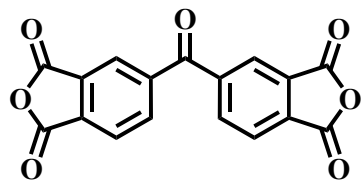
Molecular Weight = $294.22 \text{ g mol}^{-1}$

(3) The theoretical capacity of ODPA is 172 m Ah g^{-1} , where its chemical structure is as follows:



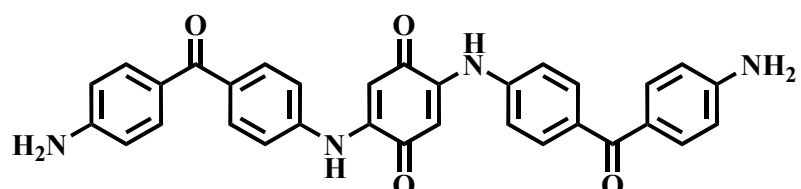
Molecular Weight = $310.22 \text{ g mol}^{-1}$

(4) The theoretical capacity of BTDA is 249 m Ah g⁻¹, where its chemical structure is as follows:



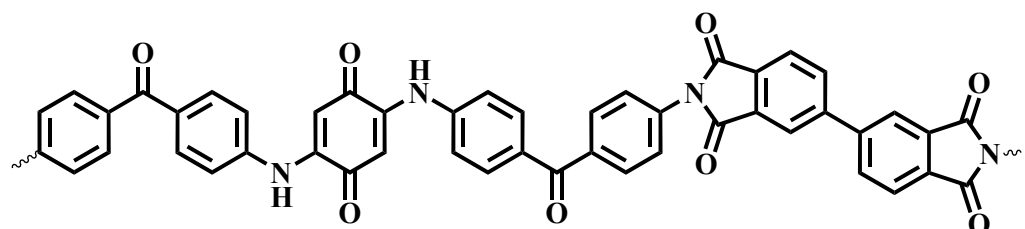
Molecular Weight = 322.23 g mol⁻¹

(5) The theoretical capacity of QDP is 202 m Ah g⁻¹, where its chemical structure is as follows:



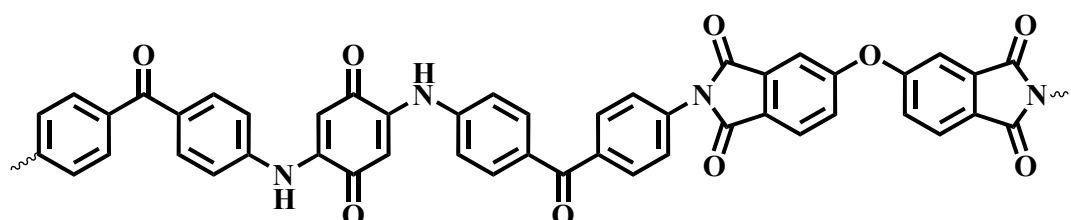
Molecular Weight = 528.57 g mol⁻¹

(6) The theoretical capacity of BPQP is 204 m Ah g⁻¹, where the chemical structure of its repeating unit is as follows:



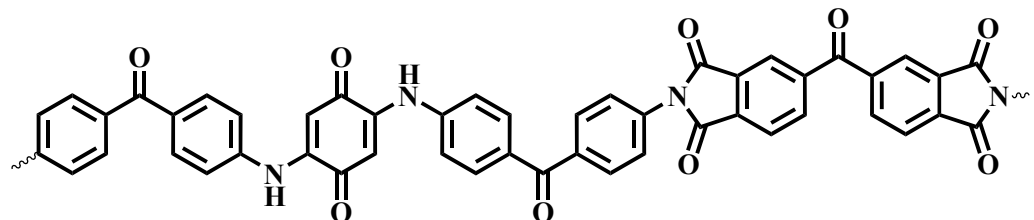
Molecular Weight = 786.76 g mol⁻¹

(7) The theoretical capacity of ODQP is 200 m Ah g⁻¹, where the chemical structure of its repeating unit is as follows:



Molecular Weight = 802.76 g mol⁻¹

(8) The theoretical capacity of BTQP is 230 m Ah g^{-1} , where the chemical structure of its repeating unit is as follows:



$$\text{Molecular Weight} = 814.77 \text{ g mol}^{-1}$$

On the other hand, the theoretical capacity of Super P is very low, about 20 m Ah g^{-1} owing to the pseudocapacitive effect or the surface adsorption, not the bulk intercalation, because it is considered a highly disordered form of carbon and treated as electrochemically inactive. Remarkably, as the number of active carbonyl groups of any organic redox material increases, its theoretical capacity increases, like BTDA and BTQP. In contrast, the theoretical capacity is inversely proportional to the molecular weight of the redox-active material according to equation (S1), proving that $C_{\text{th}}(\text{PMDA}) > C_{\text{th}}(\text{BPDA}) > C_{\text{th}}(\text{ODPA})$ as well as $C_{\text{th}}(\text{PMQP}) > C_{\text{th}}(\text{BPQP}) > C_{\text{th}}(\text{ODQP})$.



Fig. S1. The brown powder of QDP diamine product.

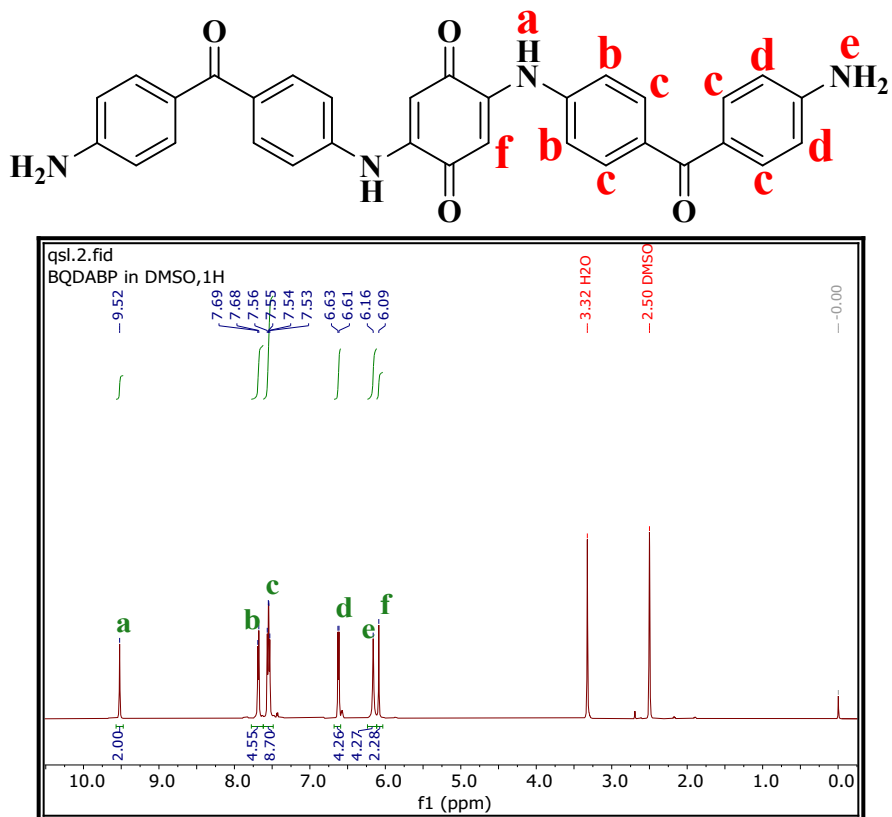


Fig. S2. The ¹H NMR spectrum of QDP diamine monomer.

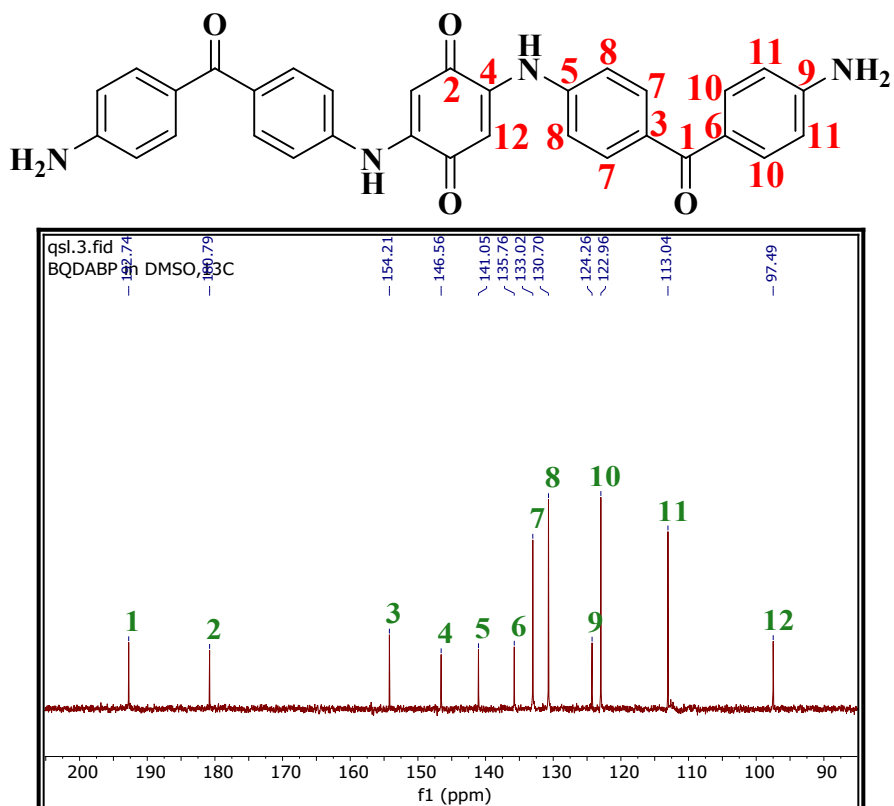


Fig. S3. The ¹³C NMR spectrum of QDP diamine monomer.

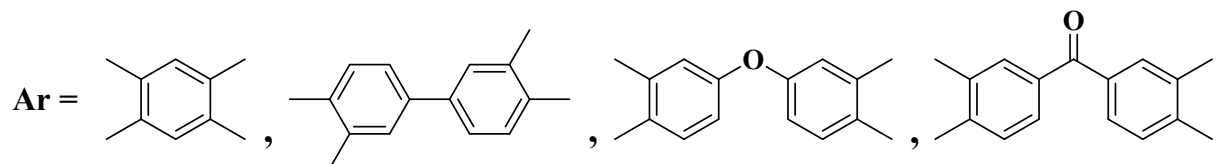
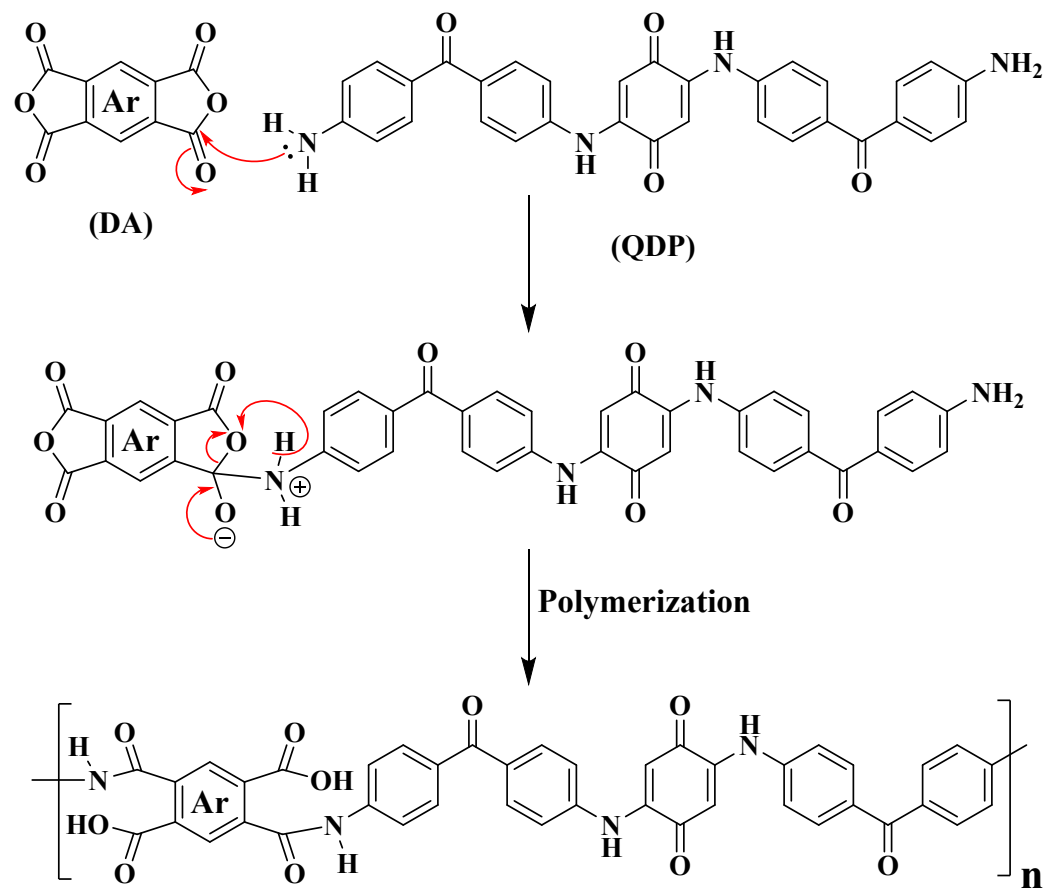


Fig. S4. The reaction mechanism of the poly(amic acid) synthesis.

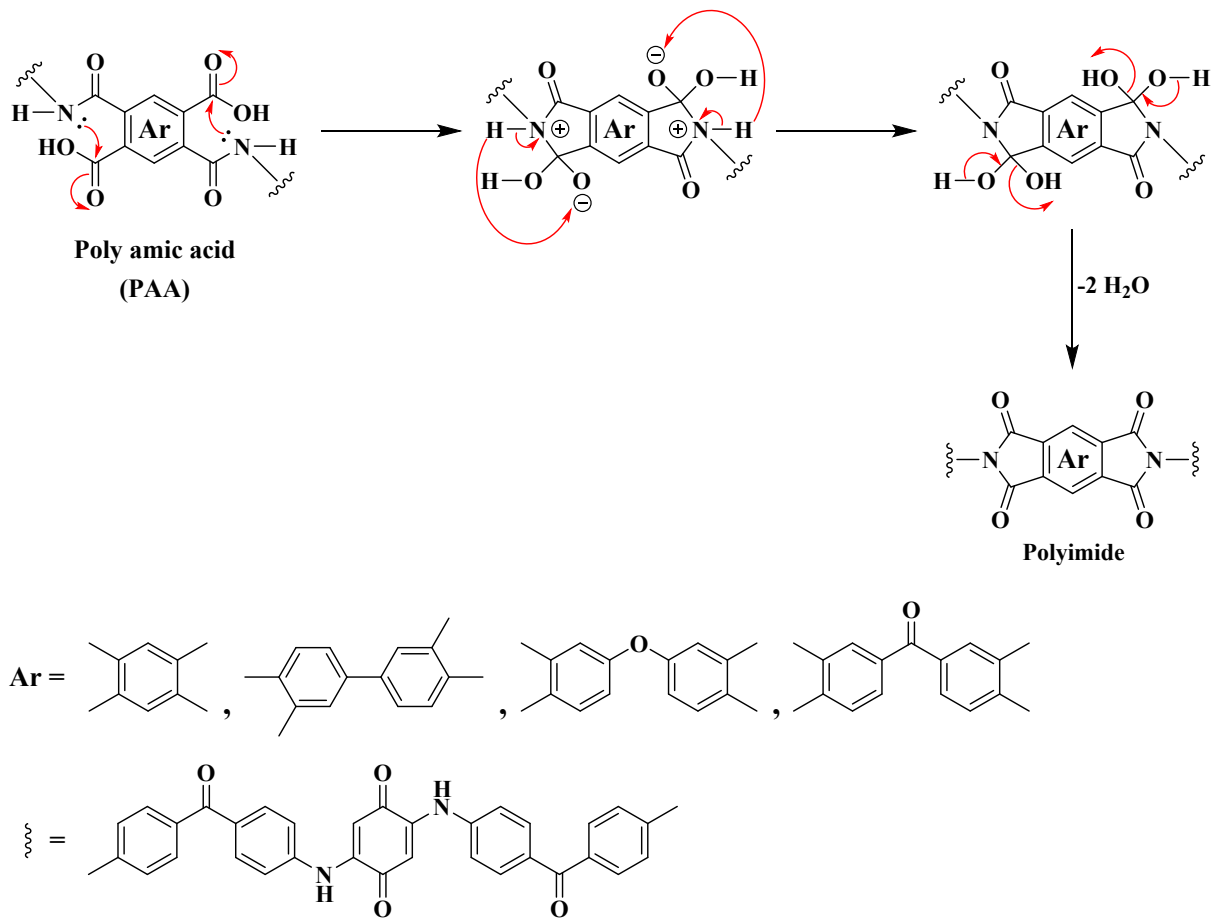


Fig. S5. A simplified mechanism for the synthesis of polyimide derivatives.

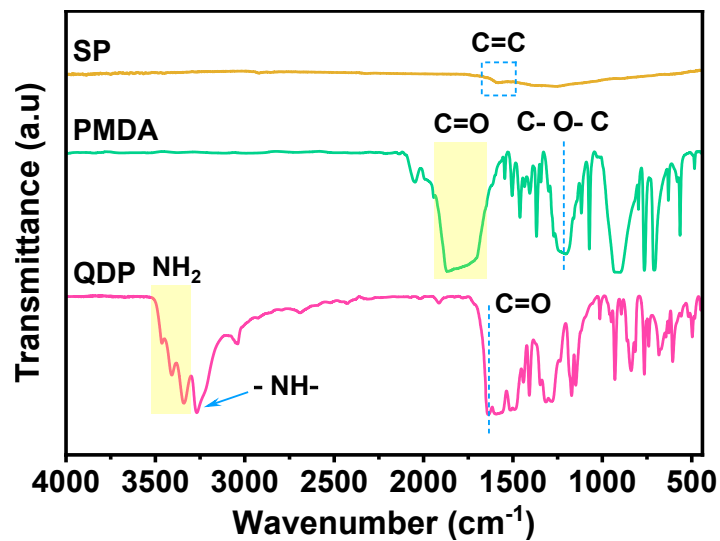


Fig. S6. FTIR spectra of QDP, PMDA, and Super C45 (SP).

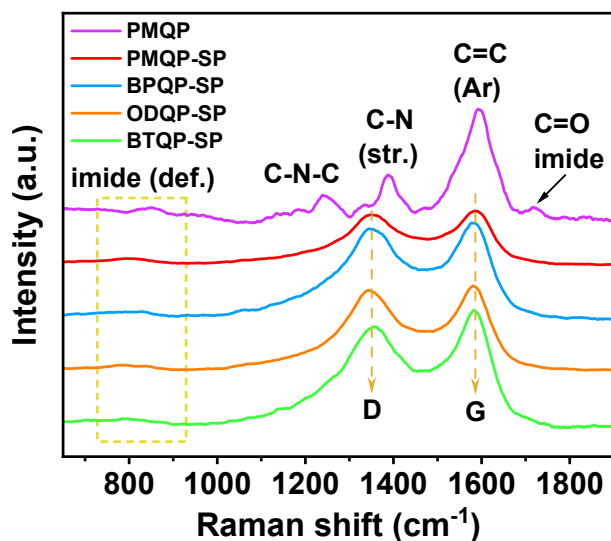


Fig. S7. Raman spectra of PMQP, PMQP-SP, BPQP-SP, ODQP-SP, and BTQP-SP polyimide composites.

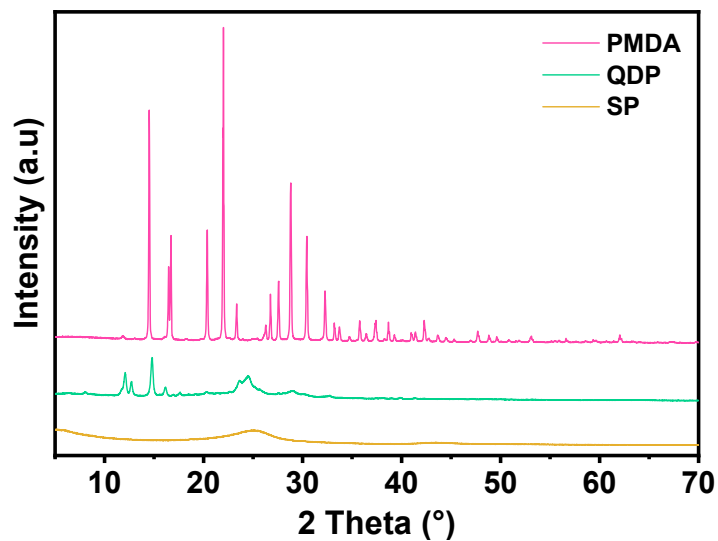


Fig. S8. XRD patterns of PMDA, QDP, and Super C45 (SP).

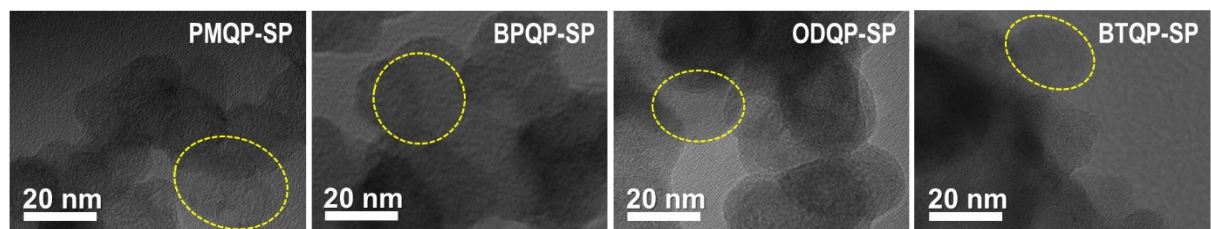


Fig. S9. TEM images of PMQP-SP, BPQP-SP, ODQP-SP, and BTQP-SP polyimide composites.

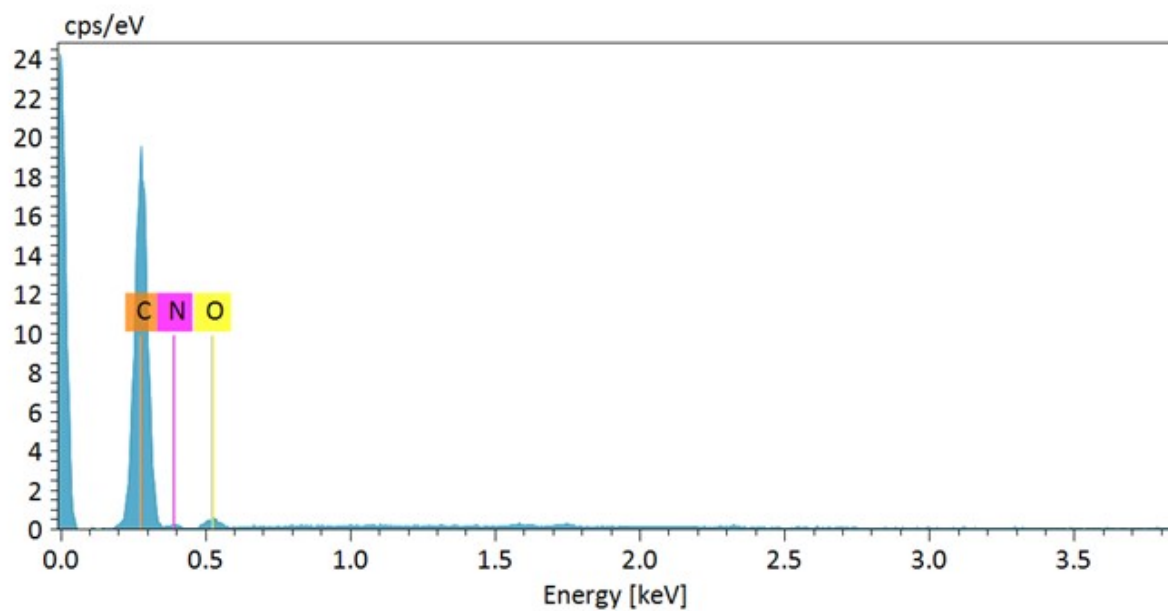


Fig. S10. EDS elemental analysis of PMQP-SP polyimide composite.

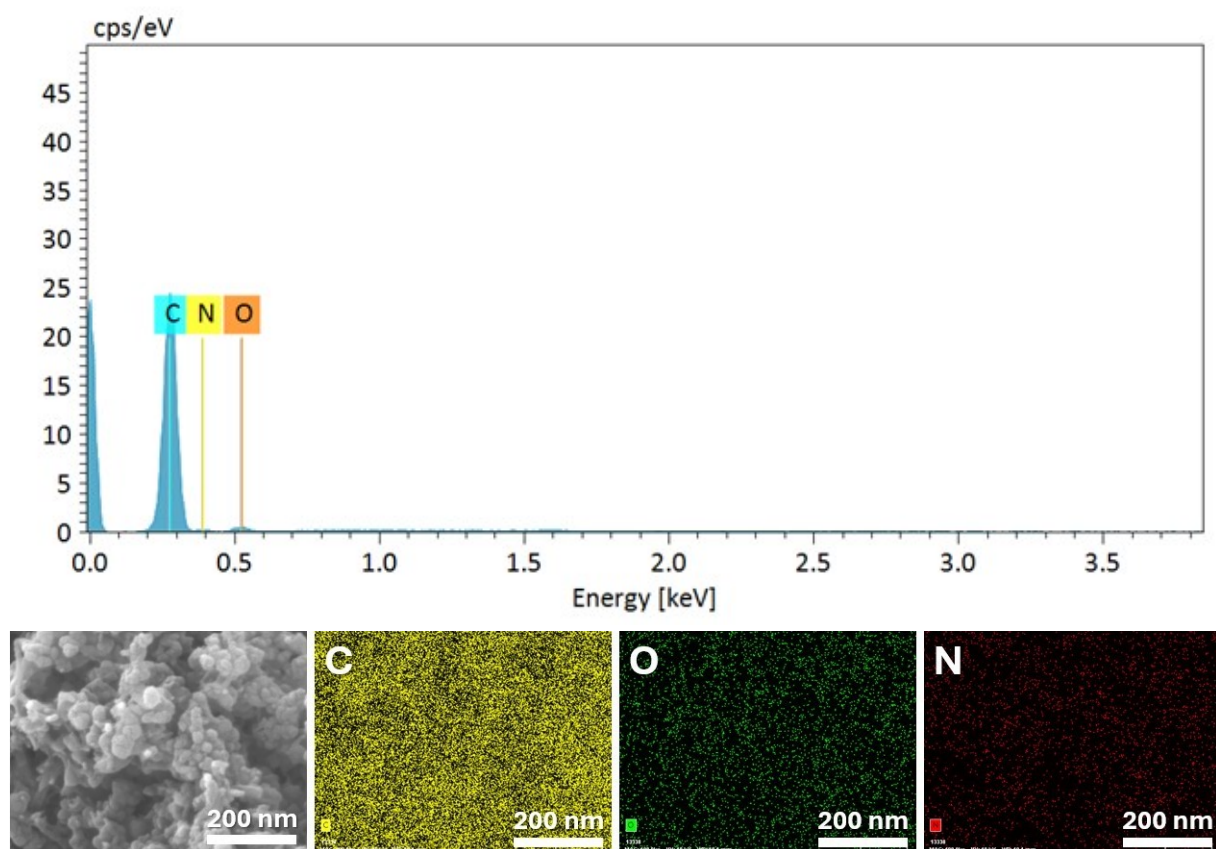


Fig. S11. EDS elemental mapping analysis of BPQP-SP polyimide composite.

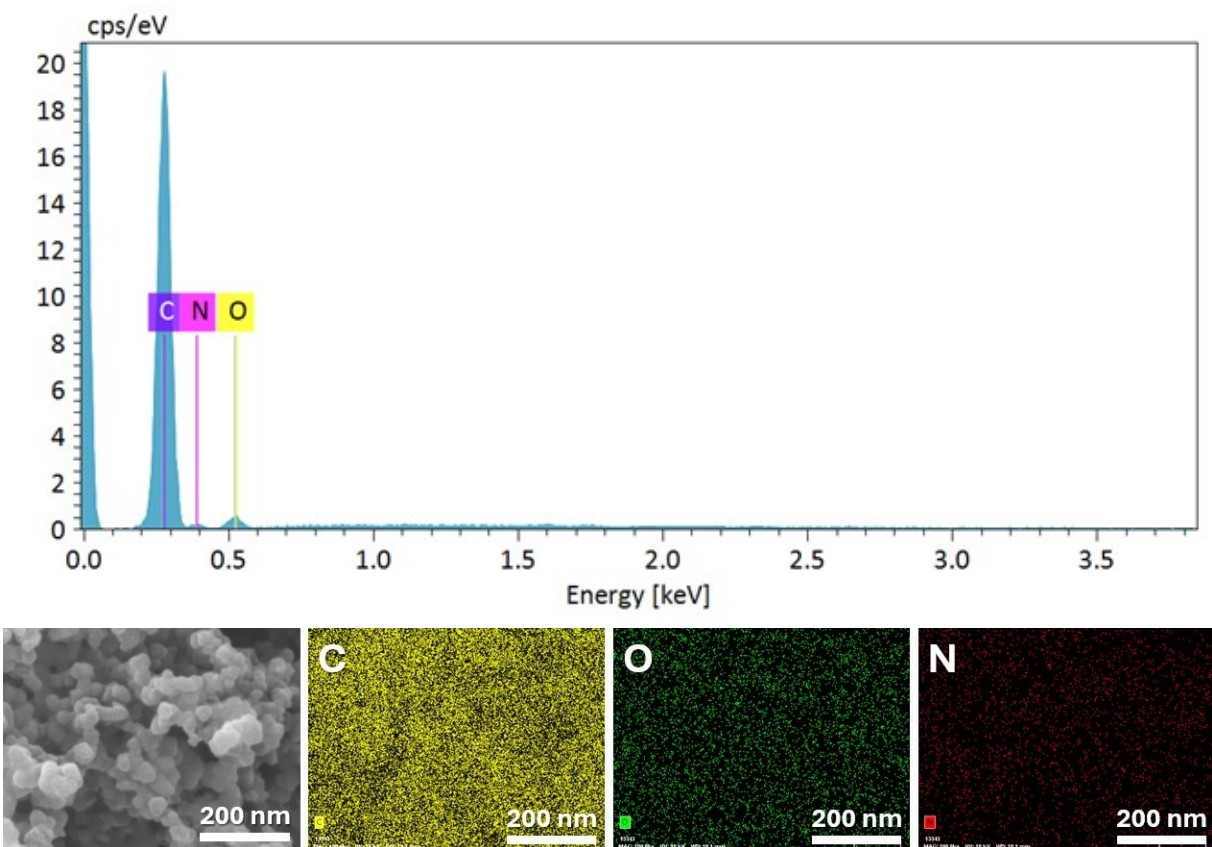


Fig. S12. EDS elemental mapping analysis of ODQP-SP polyimide composite.

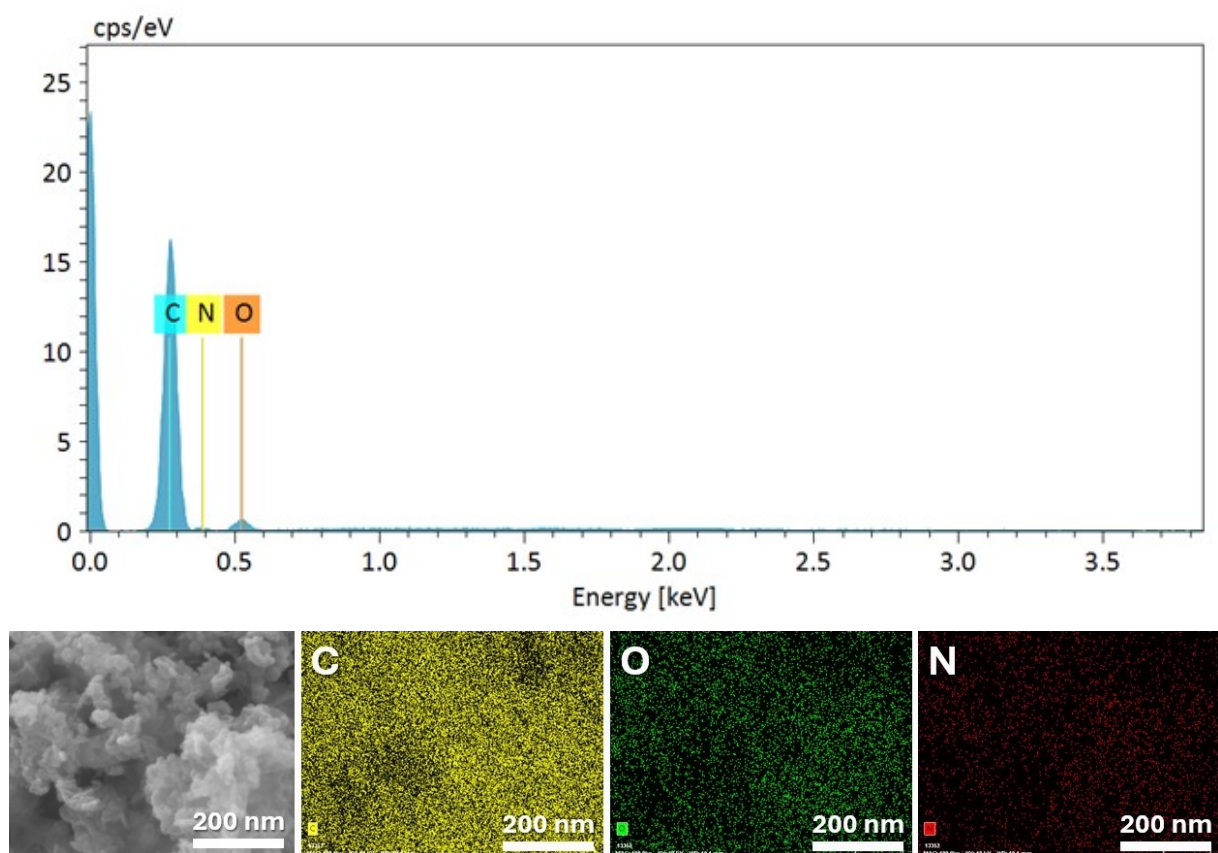


Fig. S13. EDS elemental mapping analysis of BTQP-SP polyimide composite.

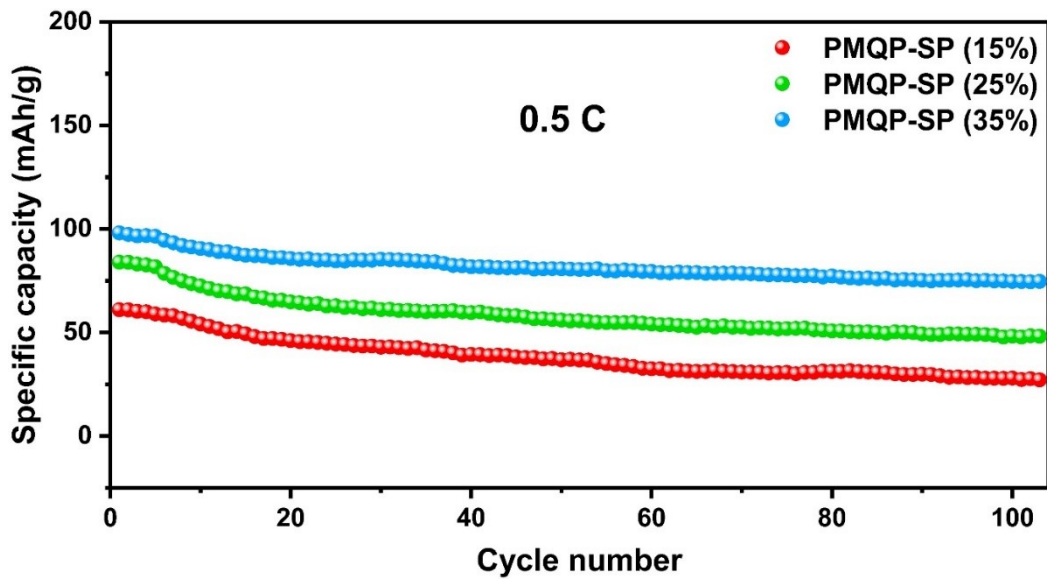


Fig. S14. Cycling performances of PMQP-SP (15%), PMQP-SP (25%), and PMQP-SP (35%) cathodes at a current density of 0.5C.

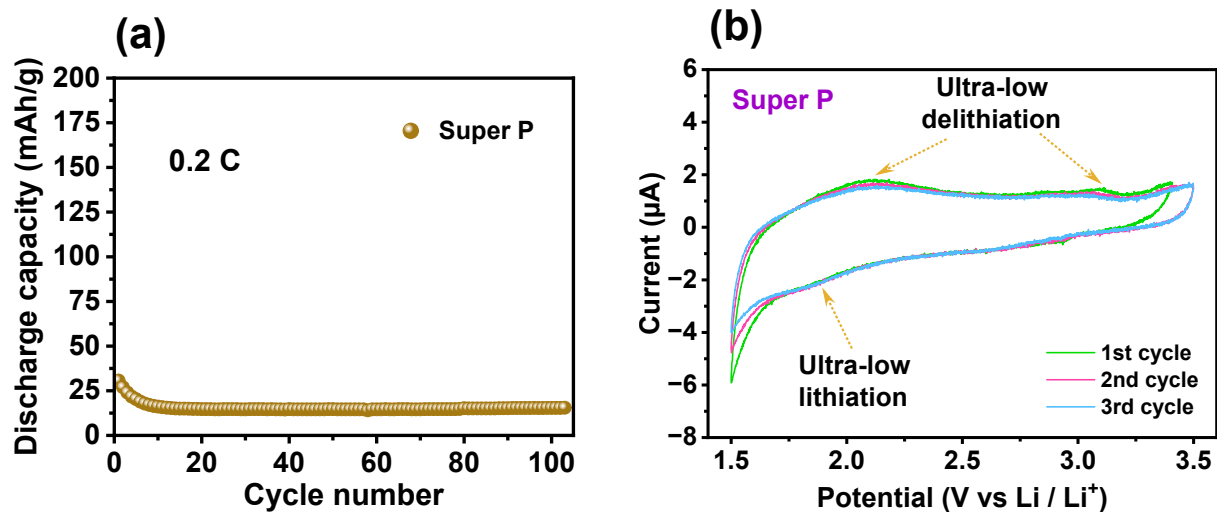


Fig. S15. (a) Cycling performance of Super P at 0.2C. (b) CV curves of Super P at a scan rate of 0.1 mV s⁻¹.

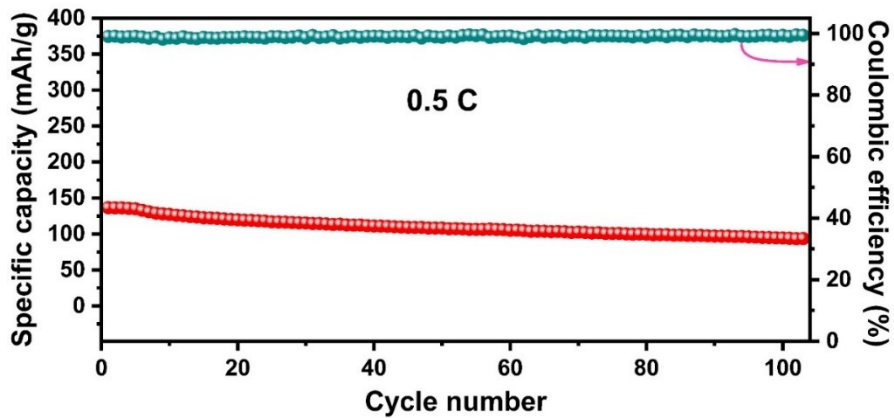


Fig. S16. Cycling performance of PMQP-SP composite at 0.5C.

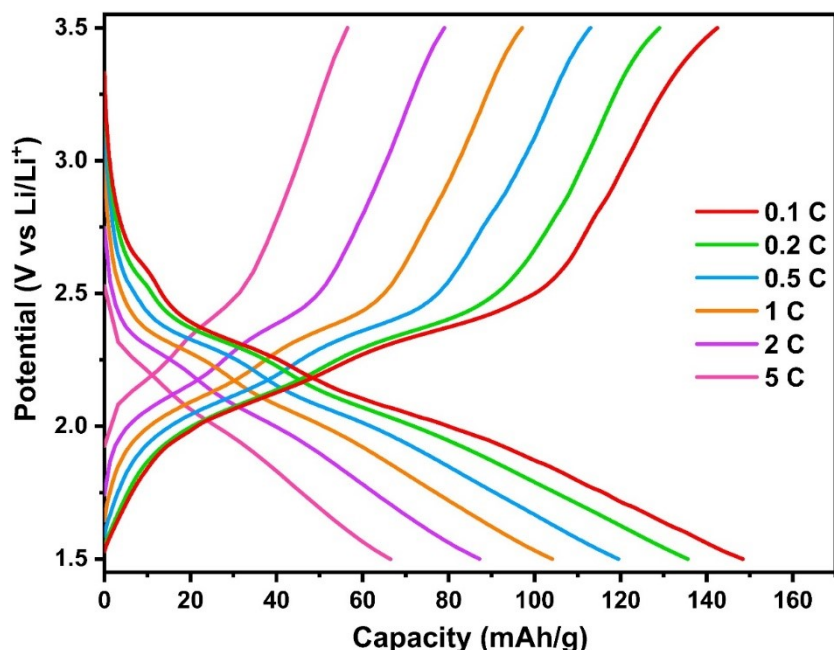


Fig. S17. Charge–discharge profiles of PMQP-SP cathode at different current densities in 1 M LiTFSI (DOL : DME) electrolyte.

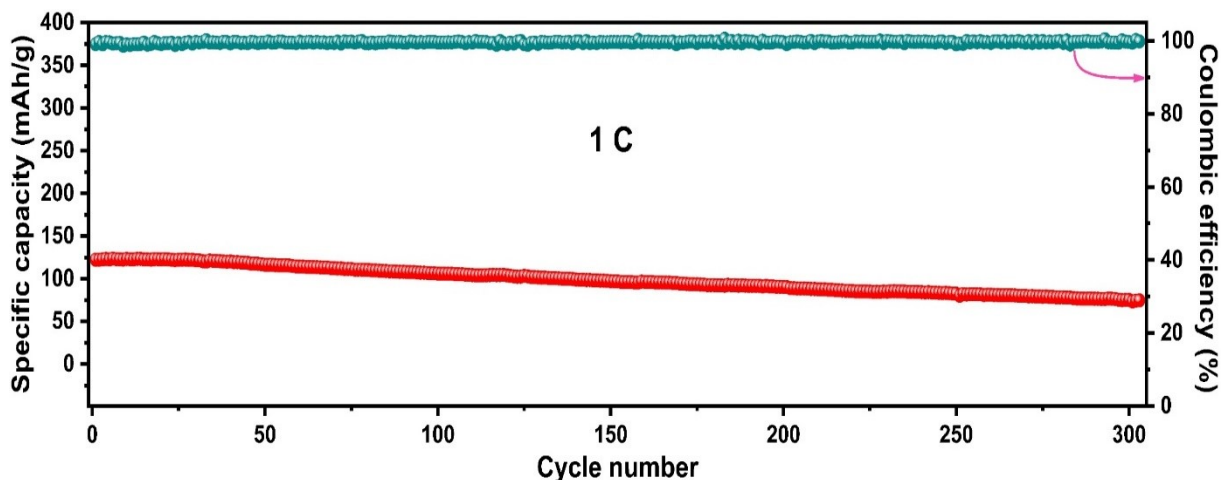


Fig. S18. Long-term cycling stability of PMQP-SP cathode at 1C.

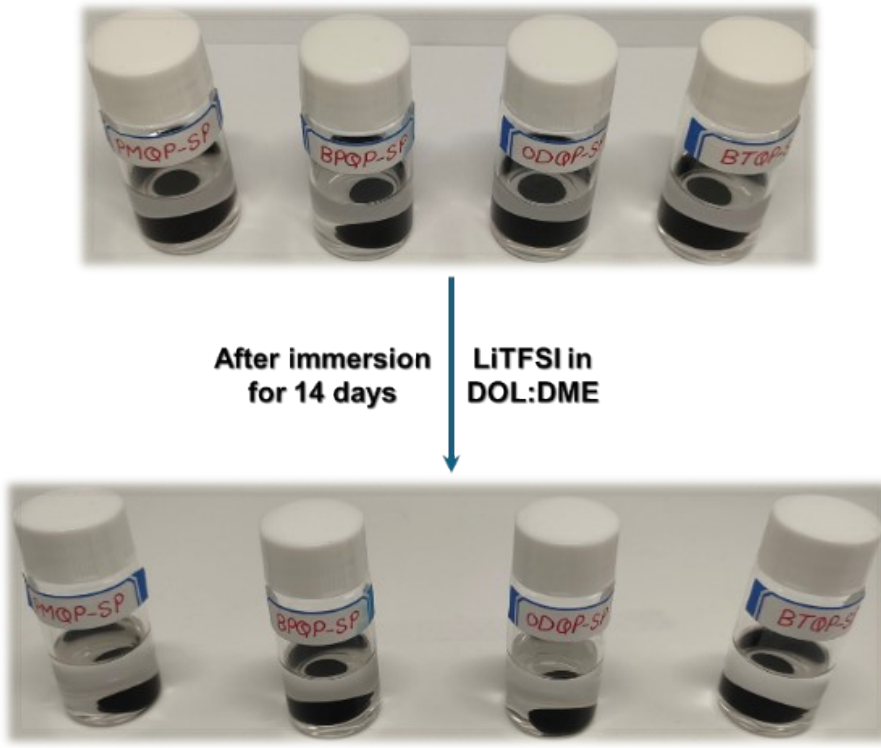


Fig. S19. Optical image of immersion of PMQP-SP, BPQP-SP, ODQP-SP, and BTQP-SP cathodes in 1 M LiTFSI (DOL : DME) electrolyte for 14 days.

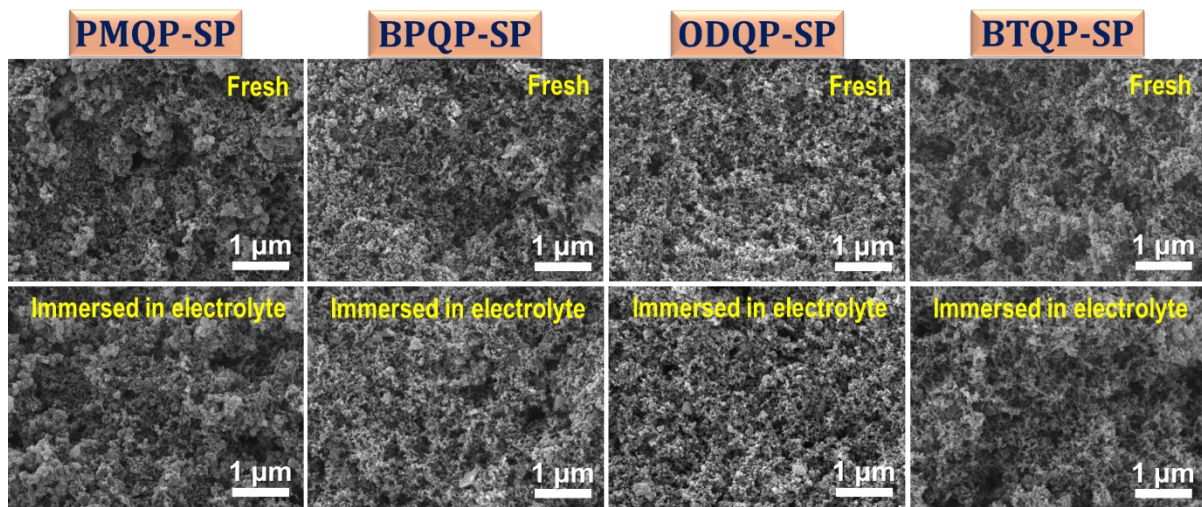


Fig. S20. SEM images of PMQP-SP, BPQP-SP, ODQP-SP, and BTQP-SP cathodes before and after immersion in 1 M LiTFSI (DOL : DME) electrolyte.

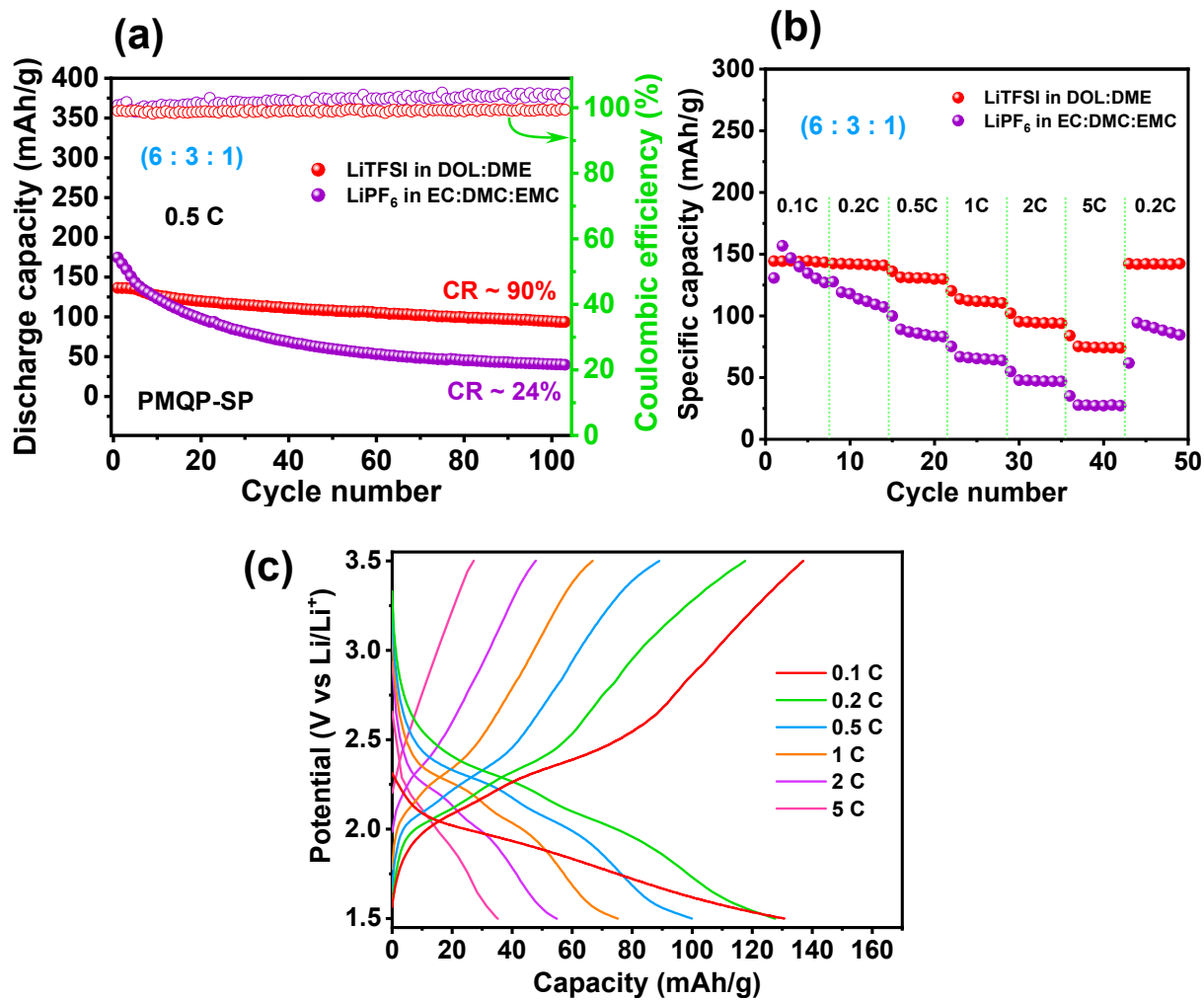


Fig. S21. Electrochemical performance of PMQP-SP cathode in different electrolytes. (a) Cycling performance at 0.5C. (b) Rate performance at different current densities. (c) Charge–discharge profiles at different current densities in 1 M LiPF₆ (EC : DME : EMC) electrolyte.

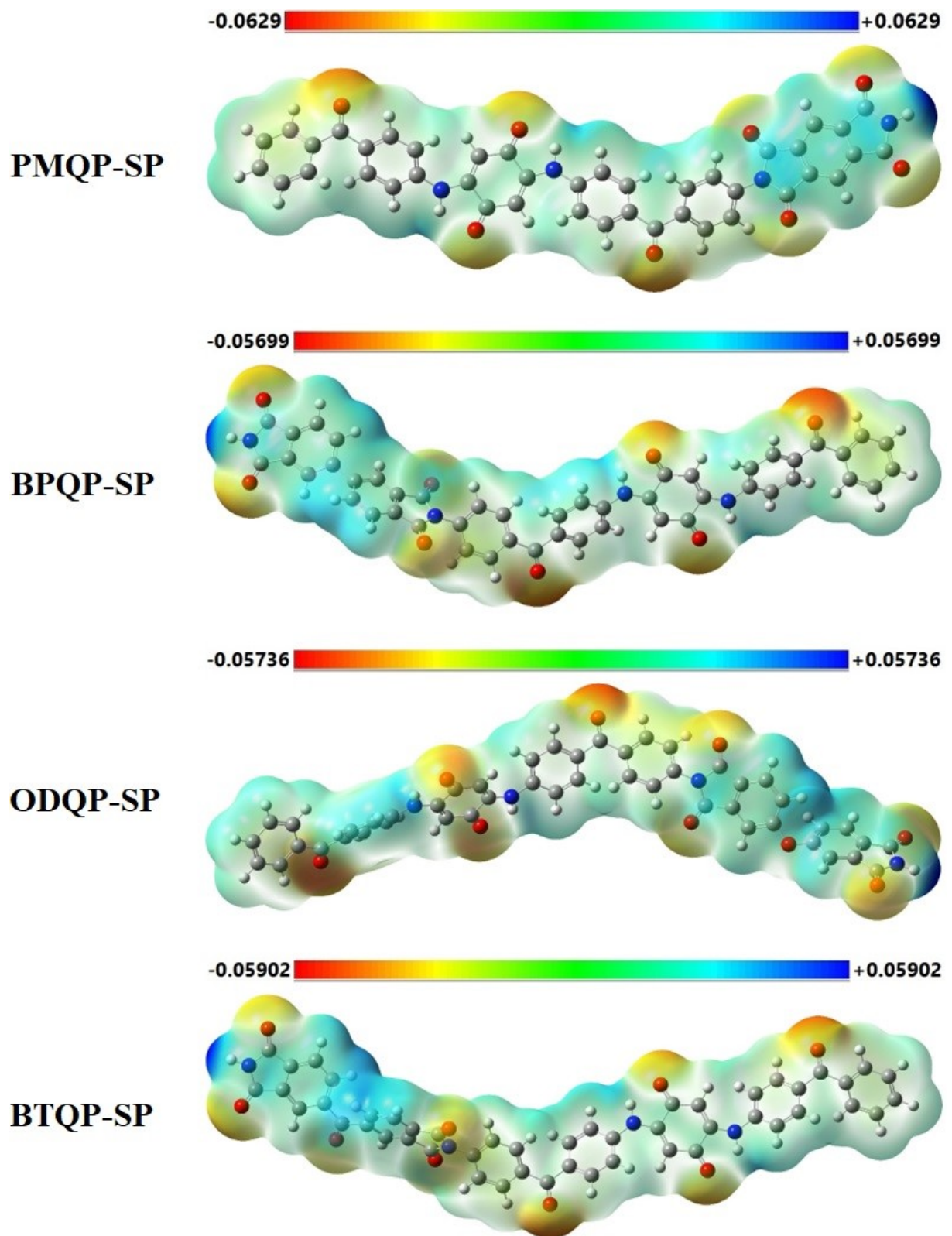


Fig. S22. The electrostatic potential surfaces of PMQP-SP, BPQP-SP, ODQP-SP, and BTQP-SP polyimide derivatives.

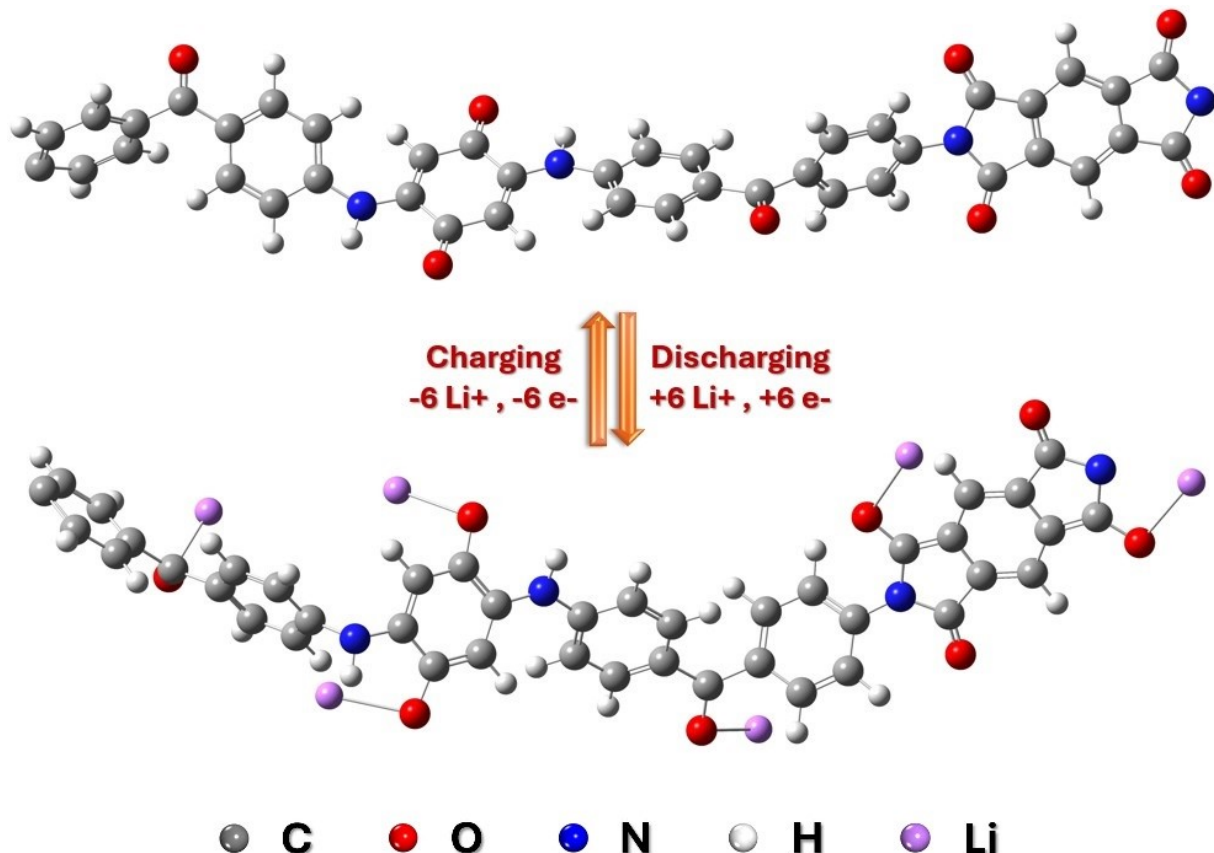


Fig. S23. 3D structural evolution of PMQP-SP during lithiation–delithiation process.

Table S1. Comparison of the battery performance based on our PMQP-SP composite cathode with other reported polyimide electrode materials.

Electrode materials	Specific capacity (mAh g ⁻¹)	Capacity retention	Electrode composition (Active material: conductive additive:binder)	Ref.
PNTCDA	90 at 0.05 C 87 at 0.5 C 80 at 1 C	100% after 32 cycles at 0.05 C	-	²
PPN	120 at 0.48 C	-	5 : 4 : 1	³
E-TP-COF	110 at 1.92 C	87.3% after 500 cycles at 1.92 C	6 : 3 : 1	⁴
PI-COF	70.6 at 0.24 C	80% after 10000 cycles at 14.4 C	5 : 4 : 1	⁵
PDI-Bz	120 at 0.24 C	46.6% after 50 cycles at 0.24 C	6 : 3 : 1	⁶
PDI-Ur	119 at 0.24 C	94.1% after 50 cycles at 0.24 C	6 : 3 : 1	⁶
PI-3	113.5 at 0.48 C	~ 100% after 3000 cycles at 9.62 C	6 : 3 : 1	⁷
2D PAI@CNT	104 at 0.96 C	100% after 8000 cycles at 4.81 C	8 : 1 : 1	⁸
NEP	127.3 at 0.19 C	-	6 : 3 : 1	⁹
Tb-DANT-COF	144 at 0.34 C	64.5% after 300 cycles at 1.4 C	6 : 2 : 2	¹⁰
PMTA-SWCNT	147 at 0.1 C	86.6% after 200 cycles at 0.5 C	6.5 : 3 : 0.5	¹¹
D _{TP} -A _{NDI} -COF@CNT _s	67 at 2.4 C	100% after 700 cycles at 2.4 C	7 : 2 : 2	¹²
PI3	132 at 0.24 C	~ 65% after 100 cycles at 1.92 C	6 : 3 : 1	¹³
PI/CNT	115 at 0.1 C	93% after 300 cycles at 0.96 C	8.5 : 1 : 0.5	¹⁴
PMQP-SP	143 at 0.2 C 136.5 at 0.5 C 122 at 1 C 97.4 at 2 C	91% after 100 cycles at 0.2 C 90% after 100 cycles at 0.5 C 89% after 300 cycles at 1 C 85% after 500 cycles at 2 C	6 : 3 : 1	Our work

References

- 1 Z. Ba, Z. Wang, M. Luo, H. Li, Y. Li, T. Huang, J. Dong, Q. Zhang and X. Zhao, *ACS Appl. Mater. Interfaces*, 2020, **12**, 807–817.
- 2 D. Monti, N. Patil, A. P. Black, D. Raptis, A. Mavrandonakis, G. E. Froudakis, I. Yousef, N. Goujon, D. Mecerreyes, R. Marcilla and A. Ponrouch, *ACS Appl. Energy Mater.*, 2023, **6**, 7250–7257.
- 3 J. Wang, H. Liu, C. Du, X. Zhang, Y. Liu, H. Yao, Z. Sun and S. Guan, *Chem. Eng. J.*, 2022, **444**, 136598.
- 4 G. Zhao, H. Li, Z. Gao, L. Xu, Z. Mei, S. Cai, T. Liu, X. Yang, H. Guo and X. Sun, *Adv. Funct. Mater.*, 2021, **31**, 2101019.
- 5 S. Lei, Y. Dong, Y. Dou, X. Zhang, Q. Zhang and Y. Yang, *Mater. Adv.*, 2021, **2**, 5785–5790.
- 6 M. Ruby Raj, R. V. Mangalaraja, D. Contreras, K. Varaprasad, M. V. Reddy and S. Adams, *ACS Appl. Energy Mater.*, 2020, **3**, 240–252.
- 7 Q. Zhang, G. Lin, Y. He, X. Cui and Y. Yang, *Mater. Today Chem.*, 2020, **17**, 100341.
- 8 G. Wang, N. Chandrasekhar, B. P. Biswal, D. Becker, S. Paasch, E. Brunner, M. Addicoat, M. Yu, R. Berger and X. Feng, *Adv. Mater.*, 2019, **31**, 1901478.
- 9 C. Chen, X. Zhao, H.-B. Li, F. Gan, J. Zhang, J. Dong and Q. Zhang, *Electrochim. Acta*, 2017, **229**, 387–395.
- 10 D.-H. Yang, Z.-Q. Yao, D. Wu, Y.-H. Zhang, Z. Zhou and X.-H. Bu, *J. Mater. Chem. A*, 2016, **4**, 18621–18627.
- 11 H. Wu, Q. Meng, Q. Yang, M. Zhang, K. Lu and Z. Wei, *Adv. Mater.*, 2015, **27**, 6504–6510.
- 12 F. Xu, S. Jin, H. Zhong, D. Wu, X. Yang, X. Chen, H. Wei, R. Fu and D. Jiang, *Sci. Rep.*, 2015, **5**, 8225.
- 13 H. Wang, S. Yuan, D. Ma, X. Huang, F. Meng and X. Zhang, *Adv. Energy Mater.*, 2014, **4**, 1301651.

14 H. Wu, K. Wang, Y. Meng, K. Lu and Z. Wei, *J. Mater. Chem. A*, 2013, **1**, 6366–6372.